Scientific Annals of Computer Science vol. 36 (1), 2026, pp. 107–138
doi: 10.47743/SACS.2026.1.107

Path Energy Bounds For Hub-Centric Graphs Of Order $2n + 1$ With Algorithmic Computation

R. Jerlinkasmir[1], J. Veninstine Vivik [2],
Ismail Naci Cangul[3], M. Venkatachalam[4]

Abstract

This study investigates the path energy bounds of hub-centric graph families of order $(2n+1)$, denoted by $\mathscr{H}_{2n+1}$. The path energy is defined as the absolute sum of the eigenvalues of the path adjacency matrix $A_p(\mathscr{H}_{2n+1})$, where each entry p_{ij} measures the maximum number of internally vertex- disjoint paths. Through an in-depth examination of the characteristic values of this matrix $A_p(\mathscr{H}_{2n+1})$, we derive path energy bounds specific to these four $(2n + 1)$-vertex graph, namely closed helm, double star, friendship, and double wheel graphs. We further developed an explicit spectral construction enabling the numerical validation algorithm to evaluate the time complexity in various structural configurations of $(2n + 1)$-graphs. Also executed extensive trials to capture their average, maximum, and minimum computational performances. This analysis offers a detailed comparative study of the structural attributes that lead to computational complexity, highlighting the substantial algorithmic demands for several graphs.

Keywords: Eigen Values, Closed Helm, Double Star, Friendship, Double Wheel, Energy, Path energy, Time complexity

This work is licensed under the Creative Commons Attribution Licence (CC BY)

[1]Department of Mathematics, M.Kumarasamy College of Engineering, Karur – 639113, Tamil Nadu, India. Email: jerlinkasmirrubancharles@gmail.com

[2]Department of Mathematics, Karunya Institute of Technology and Sciences, Karunya Nagar, Coimbatore, 641114, Tamil Nadu, India. Email: vivikjose@gmail.com

[3]Department of Mathematics, Bursa Uludag University, Ozluce Gorukle Campus, Gorukle, 16059, Bursa, Turkey. Email: cangul@uludag.edu.tr

[4]Department of Mathematics, Kongunadu Arts and Science College, Coimbatore, 641 029, Tamil Nadu, India. Email: Venkatmaths@gmail.com

1 Introduction

An undirected graph $G = (V, E)$ consists of a vertex set V and an edge set E [5]. Ivan Gutman first proposed the concept of graph energy in 1978 [10, 16], drawing ideas from the Hückel Molecular Orbital (HMO) model. Gutman's innovative extension of this model, which was initially intended to evaluate the overall energy of π-electrons in molecular structures, defined an energy measure that could be used to graphs. New perspectives on energy within a strictly mathematical framework were made possible by this adaption. There is a lot of scholarly interest in graph energy, which has returned to prominence as a key topic in chemical graph theory. Throughout its resurgence, the discipline has grown significantly, with well over hundred research articles published annually [12, 11, 16]. As a result, recent works have carefully constructed and examined a wide range of attributes and strict constraints around graph energy [4, 3, 6, 23]. The $(0, 1)$-adjacency matrix in a molecular graph G with n vertices generates eigenvalues represented by $\lambda_1, \lambda_2, \ldots, \lambda_n$, which collectively determine the graph's spectral profile. Calculating the sum of these eigenvalues' absolute values yields the idea of graph energy. The structural characteristics of G [10, 27] are reflected in this metric. Patekar et al. introduced a novel idea, the pathway matrix, in their study [20, 22], which forms the basis for the concept of path energy in graphs, extending the classical definition of graph energy to a new dimension. Let $A_p(G) = (p_{ij})$ be an $n \times n$ path adjacency matrix, where the element p_{ij} represents the maximum number of internally vertex disjoint paths connecting vertices v_i and v_j, with $i \neq j$. If $i = j$, assign p_{ij} a value of zero.

Energy patterns in paths across different graph types are thoroughly analyzed by Ilic and Milan. [14], who arrive at important conclusions about its unique features. Similarly, Raza et al. [21] investigate graph spectral properties in their 2023 study, offering insightful viewpoints on spectral patterns in various graph types. In their research, Xu and Zhou [26] analyze the kinds of graphs that, given particular structural circumstances, reach both the path index's maximum and minimum values. The study by Cvetkovski et al. [8] looks at a number of inequalities, some of which are useful for improving bounds and the precision of energy calculations in graph frameworks. Expanding upon these approaches, we provide more stringent upper and lower bounds for the path energy in graphs that satisfy the necessary conditions. Narke and Malavadkar [19] (2026), presented improved (tighter) path energy bounds and an efficient algorithm for path matrix computation. Hutter et al. [13] examined machine learning techniques for

forecasting algorithm execution durations, emphasizing unique features of particular difficulties. Simonsson et al. [24] have presented a reduced-order modeling approach based on spectral graph theory for simulating graphs in city-scale district energy grids.

Spectral complexity is a novel measure of complexity for directed graphs that was introduced by Mez and Duran [9, 17]. This new metric efficiently captures graph complexity by enabling polynomial-time computation of path matrix eigenvalues, despite the structural intricacy of the graphs.

2 Motivation and Preliminary Results

In this section, the motivation, methodology and inequalities that provide the foundation for our work are discussed.

Graph theory plays a pivotal role in the optimization of complex networks; however, computation of the path energy parameter, which serves as a crucial measure of network connectivity via vertex-independent paths, presents significant challenges. Efficient determination of path energy metrics is indispensable for the design of resilient and high-performance networks. To address the complexities involved in calculating pathway energy for intricate $(2n+1)$-networks. This paper provides a computational framework for evaluating path energy. Our approach constructs a path adjacency matrix $A_p(G)$, which encodes the maximum number of vertex-disjoint paths between distinct vertex pairs. For a G with n vertices, the path adjacency matrix $A_p(G) = (p_{ij})_{n\times n}$ by

$$p_{ij} = \begin{cases} \text{maximum number of vertex-disjoint paths from } v_i \text{ to } v_j, & i \neq j, \\ 0, & i = j. \end{cases}$$

Since $A_p(G)$ is a real symmetric matrix, all its eigen values are real. Let $\Lambda_1, \Lambda_2, \ldots, \Lambda_n$ be the eigen values of $A_p(G)$. The **Path energy** [22] of G is defined as

$$E_p(G) = \sum_{i=1}^{n} |\Lambda_i|.$$

Leveraging the eigen values, we derive a set of path energy bounds, including lower and upper bounds. Additionally, we present a computational algorithm for performing n-trial analyses to evaluate the time complexity of these graphs by computing the average, maximum, and minimum execution times. The study combines matrix-based computation and spectral analysis to

investigate the structural and complexity properties of the considered graph families. A $(\mathbf{2n+1})$-graphs refers to a class of graphs characterized by having a total of $(2n+1)$ vertices. These graphs are typically studied in graph theory due to their structural asymmetry and unique properties arising from their odd number of vertices. The following are few examples of $(2n+1)$-graphs (see Figure 1) considered in this study. The **Helm graph** H_n[15] is formed by augmenting the outer cycle C_n of a **Wheel graph** W_n with a pendant edge attached to each vertex of the cycle. By further enhancing this structure through the addition of edges that interconnect these pendant vertices, the **Closed Helm graph** CH_n [15] emerges as a refined variant of the Helm graph. A different structural transformation leads to the **Double Star graph** DS_n[15], which extends the conventional **Star graph** $K_{1,n}$ by incorporating an additional pendant edge to each existing pendant vertex, forming $K_{1,n,n}$. Expanding upon the connectivity of cyclic structures, the **Double Wheel graph** DW_n [7] consists of two cycles of size n, each fully connected to a common central hub, effectively reinforcing its structural cohesion. Further exploring networks with a shared vertex, the **Friendship graph** F_n [18] is the graph obtained by joining n copies of the cycle C_3 at a single common vertex. Equivalently, F_n consists of n triangles sharing exactly one common central vertex. Consequently, F_n has $2n+1$ vertices and $3n$ edges. The advantages of using $(2n+1)$-graphs lie in the odd

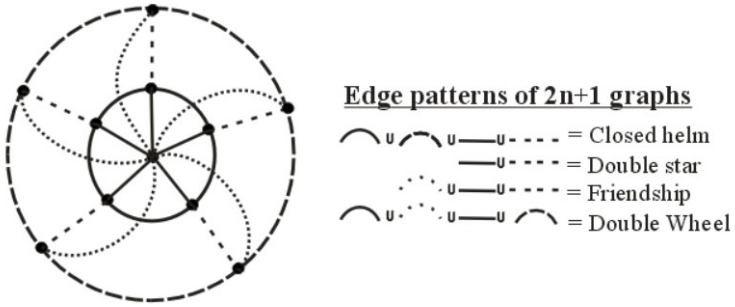

Figure 1: Generalized graph structure of CH_n, DS_n, F_n, and DW_n.

number of vertices, which introduces asymmetry in the pathways, leading to unique vertex-disjoint path structures. For instance, in social networks, this enables independent communication routes between an influencer and their followers, enhancing message delivery even under congestion. Similarly, in Peer-to-Peer (P2P) systems, it ensures robust file sharing through alternative data transfer pathways, which is possible because of alternate pathways

that exists in partial hub-centric model of $(2n+1)$-networks, eg., closed helm (See Figure 2a and 2b). In contradiction, the influencer plays a vital role in communication between the followers whose elimination discards the hub-centric model of $(2n+1)$ networks eg., DS_n, F_n and DW_n (See Figure 2c).

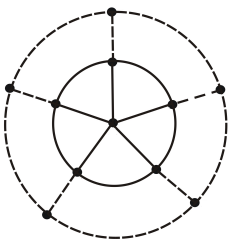

(a) The influencer hub vertex +1 helps to connect others with the followers in the inner with 4 and outer 3 disjoint pathways.

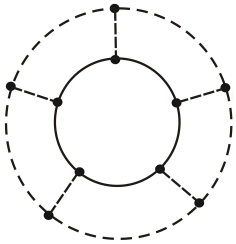

(b) After the removal of the influencer hub vertex +1 the followers stay connected with 3 disjoint pathways.

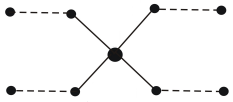

(c) The influencer hub vertex +1 plays a vital role in this non-cyclic $2n+1$ graph; without it, the connections fail.

Figure 2: Examples of $(2n+1)$-graphs with real-world analogies.

3 Characterizing the Extremal Values of Path-Based Energy in $(2n+1)$-Hub-Centric $\mathscr{H}_{2n+1}$ Graphs

This section investigates various path energy bounds for $(2n+1)$-Hub-Centric graphs, including lower bounds, exact values and upper bounds. The following proposition and matrix formulations are adopted from [2] and are used throughout the subsequent analysis.

Proposition 1. *Let $\mathscr{H}_{2n+1}$ be a connected graph of order $2n+1$, and let $\Lambda_1, \Lambda_2, \ldots, \Lambda_{2n+1}$ be the eigenvalues of the path adjacency matrix $A_p(\mathscr{H}_{2n+1})$. Then, the sum of the squares of the eigenvalues equals the sum of the squares of the distinct matrix entries a_k, each weighted by their frequencies of occurrence f_k*

$$\sum_{i=1}^{2n+1} \Lambda_i^2 = \sum_{i,j=1}^{2n+1} p_{ij}^2 = \operatorname{tr}\Big(A_p\left(\mathscr{H}_{2n+1}\right)^2\Big) = \sum_{k} a_k^2 f_k. \tag{1}$$

Remark 2. *The matrices J_n, I_n, $J_{m\times n}$, $J_{(n+1)\times n}$, and $J_{n\times(n+1)}$ are used in Propositions 3–6 to represent all-ones and identity blocks in a compact form, which simplifies the block-matrix constructions.*

$$J_n = \begin{pmatrix} 1 & 1 & \cdots & 1 \\ 1 & 1 & \cdots & 1 \\ \vdots & \vdots & \ddots & \vdots \\ 1 & 1 & \cdots & 1 \end{pmatrix}_{n\times n}, \quad I_n = \begin{pmatrix} 1 & 0 & \cdots & 0 \\ 0 & 1 & \cdots & 0 \\ \vdots & \vdots & \ddots & \vdots \\ 0 & 0 & \cdots & 1 \end{pmatrix}_{n\times n} \tag{2}$$

$$J_{n\times 1} = \begin{pmatrix} 1 \\ 1 \\ \vdots \\ 1 \end{pmatrix}_{n\times 1}, \quad J_{1\times n} = \begin{pmatrix} 1 & 1 & \cdots & 1 \end{pmatrix}_{1\times n} \tag{3}$$

$$J_{(n+1)\times n} = \begin{pmatrix} 1 & 1 & \cdots & 1 \\ 1 & 1 & \cdots & 1 \\ \vdots & \vdots & \ddots & \vdots \\ 1 & 1 & \cdots & 1 \end{pmatrix}_{(n+1)\times n} \quad J_{n\times(n+1)} = \begin{pmatrix} 1 & 1 & \cdots & 1 \\ 1 & 1 & \cdots & 1 \\ \vdots & \vdots & \ddots & \vdots \\ 1 & 1 & \cdots & 1 \end{pmatrix}_{n\times(n+1)}. \tag{4}$$

Proposition 3. *Let CH_n be the closed helm graph with $2n+1$ vertices, and if $\mu_1, \ldots, \mu_{2n+1}$ are the eigenvalues of $A_p(CH_n)$, then*

$$\sum_{i=1}^{2n+1} \Lambda_i^2 = 16(n^2+n) + 9(3n^2+n).$$

Proof. The closed helm graph CH_n contains vertex set $V = V_1 \cup V_2$ with $|V_1| = n+1$ and $|V_2| = n$. The hub vertex v_1 and the n vertices of the inner wheel constitute V_1, while the n vertices of the outer rim constitute V_2. The path connectivity between these sets determines the entries of the path adjacency matrix $A_p(CH_n)$.
The path adjacency matrix $A_p(CH_n)$ partitions as:

$$A_p(CH_n) = \begin{pmatrix} B11_{n+1\times n+1} & B12_{(n+1)\times n} \\ B21_{n\times(n+1)} & B22_{n\times n} \end{pmatrix},$$

whose the four blocks are defined as:

$$B_{11} = 4(J_{n+1} - I_{n+1}),\ B_{12} = 3J_{(n+1)\times n}\ B_{21} = 3J_{n\times(n+1)},\ B_{22} = 3(J_n - I_n).$$

Here, J_n, I_n and $J_{(n+1)\times n}$ and $J_{n\times(n+1)}$ are defined in (2) and (4).
The entries p_{ij} of the path adjacency matrix $A_p(CH_n)$ are thus:

$$p_{ij} = \begin{cases} 0, & \text{if } i = j, \\ 4, & \text{if } \{v_i, v_j\} \subseteq V_1 \text{ and } i \neq j, \\ 3, & \text{otherwise.} \end{cases}$$

Summing the non-zero entries in the block matrices:

- **Value 4:** Occurs in B_{11} corresponding to all distinct pairs within V_1. Since $|V_1| = n+1$, this yields $(n+1)^2 - (n+1) = n^2 + n$ directed adjacency. It yields to the sum $4^2(n^2+n) = 16(n^2+n)$.
- **Value 3:** Occurs in B_{12} ($(n+1)n = n^2+n$ times), B_{21} ($n(n+1) = n^2+n$ times), and the off-diagonal of B_{22} ($n^2 - n$ times). The total number of entries corresponding to value 3 is $2(n^2+n) + (n^2-n) = 3n^2 + n$. It contributes to the sum $3^2(3n^2+n) = 9(3n^2+n)$.

The total sum of squared entries is:

$$\begin{aligned} \sum_{i,j=1}^{2n+1} p_{ij}^2 &= \sum_{i=1}^{2n+1} p_{ii}^2 + \sum_{p_{ij}=4} p_{ij}^2 + \sum_{p_{ij}=3} p_{ij}^2 \; = 0 + 4^2(n^2+n) + 3^2(3n^2+n) \\ &= 16(n^2+n) + 9(3n^2+n). \end{aligned}$$

From Proposition (1), we have $\sum_{i=1}^{2n+1} \Lambda_i^2 = \sum_{i,j=1}^{2n+1} p_{ij}^2$. Thus,

$$\sum_{i=1}^{2n+1} \Lambda_i^2 = 16(n^2+n) + 9(3n^2+n).$$

Hence, the theorem is proved. □

Proposition 4. *Let DS_n be the double star graph with $2n+1$ vertices, and if $\Lambda_1, \ldots, \Lambda_{2n+1}$ are the eigenvalues of $A_p(DS_n)$, then*

$$\sum_{i=1}^{2n+1} \Lambda_i^2 = 2n(2n+1).$$

Proof. The double star graph DS_n is a tree of order $2n+1$. Let its vertex set be partitioned as $V = V_1 \cup V_2$ with $|V_1| = n+1$ and $|V_2| = n$. By the

fundamental properties of trees, there is exactly one unique path between any two distinct vertices. Therefore, the maximum number of internally vertex-disjoint paths between any $v_i, v_j \in V$ $(i \neq j)$ is exactly one.
The path adjacency matrix $A_p(DS_n)$ partitions as:

$$A_p(DS_n) = \begin{pmatrix} B11_{n+1\times n+1} & B12_{(n+1)\times n} \\ B21_{n\times(n+1)} & B22_{n\times n} \end{pmatrix},$$

whose the four blocks are defined as:

$$B_{11} = J_{n+1} - I_{n+1}, \quad B_{12} = J_{(n+1)\times n} \quad B_{21} = J_{n\times(n+1)} \quad B_{22} = J_n - I_n.$$

Here, J_n, I_n and $J_{(n+1)\times n}$ and $J_{n\times(n+1)}$ are defined in (2) and (4). Every distinct pair of vertices is connected by exactly one path, the entries p_{ij} of $A_p(DS_n)$ simplify to:

$$p_{ij} = \begin{cases} 0, & \text{if } i = j, \\ 1, & \text{if } i \neq j. \end{cases}$$

Summing the non-zero entries in the block matrices:

- **Value 1:** All off-diagonal entries in B_{11}, all entries in B_{12} and B_{21}, and the off-diagonal entries in B_{22} are equal to 1.
  The total number of entries corresponding to value 1 is
  $(n^2+n) + 2(n^2+n) + (n^2-n) = 2n(2n+1)$.

The total sum of squared entries is:

$$\sum_{i,j=1}^{2n+1} p_{ij}^2 = \sum_{i=1}^{2n+1} p_{ii}^2 + \sum_{i\neq j} p_{ij}^2 = 0 + 1^2\,(2n(2n+1)) = 2n(2n+1).$$

By proposition (1), $\sum_{i=1}^{2n+1} \Lambda_i^2 = \sum_{i,j=1}^{2n+1} p_{ij}^2$. Hence, we obtain:

$$\sum_{i=1}^{2n+1} \Lambda_i^2 = 2n(2n+1).$$

This completes the proof. □

Proposition 5. *Let F_n be the friendship graph with $2n+1$ vertices, and if $\Lambda_1, \ldots, \Lambda_{2n+1}$ are the eigenvalues of $A_p(F_n)$, then*

$$\sum_{i=1}^{2n+1} \Lambda_i^2 = 24n + 4n(n-1).$$

Proof. The friendship graph F_n consists of n disjoint pairs of vertices, each connected to a common central vertex. Let the vertex set be partitioned as $V = V_1 \cup V_2$, where $V_1 = \{v_1\}$ is the hub vertex ($|V_1| = 1$) and $V_2 = \{v_2, \ldots, v_{2n+1}\}$ contains the remaining $2n$ vertices. The number of internally vertex-disjoint paths between vertex pairs is:

- Two paths between the hub v_1 and any vertex in V_2.
- Two paths between paired vertices in V_2.
- One path through the hub v_1 to the vertices in non-adjacent vertices in V_2.

The path adjacency matrix $A_p(F_n)$ is partitioned as:

$$A_p(F_n) = \begin{pmatrix} B11_{n+1\times n+1} & B12_{(n+1)\times n} \\ B21_{n\times(n+1)} & B22_{n\times n} \end{pmatrix},$$

where the blocks are given by

$$B_{11} = \begin{pmatrix} 0 & 2J_{1\times n} \\ 2J_{n\times 1} & J_n - I_n + \mathbb{P}_n \end{pmatrix}_{(n+1)\times(n+1)}, \quad B_{12} = \begin{pmatrix} 2J_{1\times n} \\ J_n \end{pmatrix}_{(n+1)\times n},$$

$$B_{21} = \begin{pmatrix} 2J_{n\times 1} & J_n \end{pmatrix}_{n\times(n+1)}, \quad B_{22} = J_n - I_n + \mathbb{P}_n \in \mathbb{R}^{n\times n}.$$

Here $\mathbb{P}_n$ is the pairing matrix, whose entries are

$$\mathbf{p}_{ij} = \begin{cases} 1, & \text{if } i = 2k-1,\ j = 2k \text{ or } i = 2k,\ j = 2k-1, \quad k = 1, 2, 3, \ldots, \left\lfloor \frac{n}{2} \right\rfloor, \\ 0, & \text{otherwise.} \end{cases}$$

$$\mathbb{P}_n = \begin{pmatrix} \boxed{\begin{matrix} 0 & 1 \\ 1 & 0 \end{matrix}} & 0 & \cdots & 0 \\ 0 & \boxed{\begin{matrix} 0 & 1 \\ 1 & 0 \end{matrix}} & \cdots & 0 \\ \vdots & \vdots & \ddots & \vdots \\ 0 & 0 & \cdots & \boxed{\begin{matrix} 0 & 1 \\ 1 & 0 \end{matrix}} \end{pmatrix}_{n\times n}. \tag{5}$$

Here, J_n, I_n, $J_{n\times 1}$, $J_{1\times n}$, and $\mathbb{P}_n$ are defined in (2), (3) and (5). The entries p_{ij} of the path adjacency matrix $A_p(F_n)$ are defined by their block partitions:

$$p_{ij} = \begin{cases} 0, & i = j, \\ 2, & i = 0 \text{ or } j = 0, \\ 2, & \text{if } i, j \text{ are paired vertices}, \\ 1, & \text{otherwise.} \end{cases}$$

Summing the non-zero entries in the block matrices:

- **Value 2:** Occurs in Block B_{12} ($1 \times 2n = 2n$ times) and B_{21} ($2n \times 1 = 2n$ times), corresponding to central connections. It also appears in B_{22} at the $2n$ non-zero entries of P_n. The total number of entries corresponding to value 2 is $6n$.
  It yields to the sum $2^2(6n) = 24n$.
- **Value 1:** Occurs in Block B_{22} for all remaining off-diagonal positions. The total number of off-diagonal entries in B_{22} is $(2n)^2 - 2n$. Excluding the $2n$ entries corresponding to P_n, the number of entries corresponding to value 1 is
  $4n^2 - 4n = 4n(n-1)$. It yields to the sum $1^2(4n(n-1)) = 4n(n-1)$.

The total sum of squared entries is:

$$\begin{aligned} \sum_{i,j=1}^{2n+1} p_{ij}^2 &= \sum_{i=1}^{2n+1} p_{ii}^2 + \sum_{p_{ij}=2} p_{ij}^2 + \sum_{p_{ij}=1} p_{ij}^2 = 0 + 2^2(6n) + 1^2(4n(n-1)) \\ &= 24n + 4n(n-1). \end{aligned}$$

Using Proposition (1), $\sum_{i=1}^{2n+1} \Lambda_i^2 = \sum_{i,j=1}^{2n+1} p_{ij}^2$, substituting the corresponding values, we obtain

$$\sum_{i=1}^{2n+1} \Lambda_i^2 = 24n + 4n(n-1).$$

Hence, the theorem is proved. □

Proposition 6. *Let DW_n be the double wheel graph with $2n+1$ vertices, and if $\Lambda_1, \ldots, \Lambda_{2n+1}$ are the eigenvalues of $A_p(DW_n)$, then*

$$\sum_{i=1}^{2n+1} \Lambda_i^2 = 18n(n+1) + 2n^2.$$

Proof. The double wheel graph DW_n consists of a single hub vertex connected to two disjoint outer cycles (rims) of order n. Let the vertex set be partitioned as $V = \{v_1\} \cup V_1 \cup V_2$, where v_1 is the central hub, V_1 contains the n vertices of the first rim, and V_2 contains the n vertices of the second rim.
Based on the connectivity of DW_n, the number of internally vertex-disjoint paths between pairs is:

- Exactly three paths between the hub v_1 and any vertex in V_1 or V_2.
- Exactly three paths between any two distinct vertices within the same rim (V_1 or V_2).
- Exactly one path through the hub v_1 to any vertex in V_1 and any vertex in V_2.

The path adjacency matrix $A_p(DW_n)$ partitions as:

$$A_p(DW_n) = \begin{pmatrix} B_{11}{}_{(n+1)\times(n+1)} & B_{12}{}_{(n+1)\times n} \\ B_{21}{}_{n\times(n+1)} & B_{22}{}_{n\times n} \end{pmatrix}.$$

The four blocks are defined as:

$$B_{11} = 3\left(J_{n+1} - I_{n+1}\right), \quad B_{12} = \begin{pmatrix} 3J_{1\times n} \\ J_n \end{pmatrix}_{(n+1)\times n},$$

$$B_{21} = \begin{pmatrix} 3J_{n\times 1} & J_n \end{pmatrix}_{n\times(n+1)}, \quad \text{and} \quad B_{22} = 3(J_n - I_n).$$

Here, J_n, I_n, $J_{n\times 1}$, $J_{1\times n}$, $J_{(n+1)\times n}$ and $J_{n\times(n+1)}$ are defined in (2), (3) and (4). The entries p_{ij} of the path adjacency matrix $A_p(DW_n)$ are thus defined by their block partitions:

$$p_{ij} = \begin{cases} 0, & \text{if } i = j, \\ 3, & \text{if } i \neq j \text{ and } (v_i = v_1 \text{ or } v_j = v_1), \\ 3, & \text{if } i \neq j \text{ and } (\{v_i, v_j\} \subseteq V_1 \text{ or } \{v_i, v_j\} \subseteq V_2), \\ 1, & \text{otherwise.} \end{cases}$$

Summing the non-zero entries in the block matrices:

- **Value 3:** Occurs in the hub-to-rim sub matrices $B_{12}, B_{21}, B_{13}, B_{31}$ (each contributing n entries, for a total of $4n$). It also occurs in

the intra-rim sub matrices B_{22} and B_{33} (each containing $n^2 - n$ off-diagonal entries, for a total of $2n^2 - 2n$). The total number of entries corresponding to value 3 is
$4n + 2n^2 - 2n = 2n^2 + 2n = 2n(n+1)$.
Its contribution to the sum is $3^2(2n(n+1)) = 18n(n+1)$.

- **Value 1:** Occurs strictly in the inter-rim sub matrices B_{23} and B_{32}. Each is an $n \times n$ all-ones matrix, containing n^2 entries. The total number of entries corresponding to value 1 is $2n^2$. Its contribution to the sum is $1^2(2n^2) = 2n^2$.

The total sum of squared entries is:

$$\sum_{i,j=1}^{2n+1} p_{ij}^2 = \sum_{i=1}^{2n+1} p_{ii}^2 + \sum_{p_{ij}=3} p_{ij}^2 + \sum_{p_{ij}=1} p_{ij}^2 = 0 + 3^2(2n(n+1)) + 1^2(2n^2)$$
$$= 18n(n+1) + 2n^2.$$

By applying Proposition (1), we obtain

$$\sum_{i=1}^{2n+1} \Lambda_i^2 = \sum_{i,j=1}^{2n+1} p_{ij}^2 = 18n(n+1) + 2n^2.$$

Hence, the theorem is proved. □

4 Generalized Lower Bound for Path Energy of Hub-Centric Graphs $(\mathscr{H}_{2n+1})$

Theorem 7. *Let $\mathscr{H}_{2n+1}$ be Hub-Centric graphs with path-adjacency matrix $A_p(\mathscr{H}_{2n+1})$, eigenvalues as $\Lambda_1, \ldots, \Lambda_{2n+1}$, and determinant $D = |\det A_p(\mathscr{H}_{2n+1})|$. Then the lower bound for the path energy is*

$$E_p(\mathscr{H}_{2n+1}) \geq \sqrt{\sum_{i=1}^{k} |\Lambda_i|^2 + k(k-1)D^{\frac{2}{k}}}, \text{ where } k = 2n+1. \tag{6}$$

Proof. Let $\Lambda_1, \Lambda_2, \ldots, \Lambda_k$ be the eigenvalues of the path-adjacency matrix $A_p(\mathscr{H}_{2n+1})$ of a hub-centric graph with order $k = 2n+1$. The path energy

is defined as

$$E_p\left(\mathscr{H}_{2n+1}\right) = \sum_{i=1}^{k} |\Lambda_i|. \tag{7}$$

Squaring (7), we obtain

$$\left[E_p\left(\mathscr{H}_{2n+1}\right)\right]^2 = \left(\sum_{i=1}^{k} |\Lambda_i|\right)^2. \tag{8}$$

Expanding (8),we get

$$\left[E_p\left(\mathscr{H}_{2n+1}\right)\right]^2 = \sum_{i=1}^{k} |\Lambda_i|^2 + \sum_{i\neq j} |\Lambda_i||\Lambda_j|. \tag{9}$$

Applying the AM-GM inequality [8] to the $k(k-1)$ non-negative terms $\{|\Lambda_i||\Lambda_j| : i \neq j\}$ gives

$$\sum_{\substack{i,j=1 \\ i\neq j}}^{k} |\Lambda_i||\Lambda_j| \geq k(k-1) \left(\prod_{\substack{i,j=1 \\ i\neq j}}^{k} |\Lambda_i||\Lambda_j|\right)^{\frac{1}{k(k-1)}}. \tag{10}$$

The product factorizes as

$$\prod_{\substack{i,j=1 \\ i\neq j}}^{k} |\Lambda_i||\Lambda_j| = \prod_{i=1}^{k} |\Lambda_i|^{2(k-1)} = \left(\prod_{i=1}^{k} |\Lambda_i|\right)^{2(k-1)}. \tag{11}$$

Substituting (11) into (10) and then into (9), we obtain

$$\left[E_p\left(\mathscr{H}_{2n+1}\right)\right]^2 \geq \sum_{i=1}^{k} |\Lambda_i|^2 + k(k-1) \left(\prod_{i=1}^{k} |\Lambda_i|\right)^{\frac{2}{k}}. \tag{12}$$

Since $\prod_{i=1}^{k} |\Lambda_i| = |\det A_p\left(\mathscr{H}_{2n+1}\right)| = D$, equation (12) becomes

$$\left[E_p\left(\mathscr{H}_{2n+1}\right)\right]^2 \geq \sum_{i=1}^{k} |\Lambda_i|^2 + k(k-1)D^{\frac{2}{k}}. \tag{13}$$

Taking square roots on both sides yields the lower bound

$$E_p\left(\mathscr{H}_{2n+1}\right) \geq \sqrt{\sum_{i=1}^{k} |\Lambda_i|^2 + k(k-1)D^{\frac{2}{k}}} \tag{14}$$

completes the proof. □

5 Generalized Path Energy Upper Bound for Hub-Centric Graphs $\mathscr{H}_{2n+1}$

Theorem 8. *Let $\mathscr{H}_{2n+1}$ be a Hub-Centric graph having $2n+1$ vertices and let $A_p(\mathscr{H}_{2n+1})$ denote its path adjacency matrix of order $k = 2n+1$, with eigenvalues $\Lambda_1, \ldots, \Lambda_k$. Then the upper bound of path energy is defined by*

$$E_p(\mathscr{H}_{2n+1}) \leq \sqrt{8 \sum_{i=1}^{k} |\Lambda_i|^2}.$$

Proof. By the definition of path energy,

$$E_p(\mathscr{H}_{2n+1}) = \sum_{i=1}^{k} |\Lambda_i|. \tag{15}$$

Applying the Cauchy–Schwarz Inequality [8],

$$\left(\sum_{i=1}^{k} a_i b_i \right)^2 \leq \left(\sum_{i=1}^{k} a_i^2 \right) \left(\sum_{i=1}^{k} b_i^2 \right),$$

with the choices of $a_i = 1$ and $b_i = \sqrt{\frac{8}{k}}\,|\Lambda_i|$ is derived empirically to tighten the bounds. It holds true for any n. Then,

$$\left(\sum_{i=1}^{k} |\Lambda_i| \right)^2 = \left(\sum_{i=1}^{k} 1 \cdot |\Lambda_i| \right)^2 \leq \left(\sum_{i=1}^{k} 1^2 \right) \left(\sum_{i=1}^{k} \left(\sqrt{\frac{8}{k}}\,|\Lambda_i| \right)^2 \right).$$

Hence,

$$[E_p(\mathscr{H}_{2n+1})]^2 \leq k \cdot \frac{8}{k} \sum_{i=1}^{k} |\Lambda_i|^2 = 8 \sum_{i=1}^{k} |\Lambda_i|^2,$$

where $\sum_{i=1}^{k} |\Lambda_i|^2$ is taken from (1). Taking square roots yields

$$E_p(\mathscr{H}_{2n+1}) \leq \sqrt{8 \sum_{i=1}^{k} |\Lambda_i|^2}. \tag{16}$$

This completes the proof. □

Remark 9. *The path energy bounds for $\mathscr{H}_{2n+1}$ is generalized as*

$$\sqrt{\sum_{i=1}^{2n+1} |\Lambda|^2 + (2n+1)(2n)D^{\frac{2}{2n+1}}} \leq E_p\left(\mathscr{H}_{2n+1}\right) \leq \sqrt{8\sum_{i=1}^{2n+1} |\Lambda|^2}. \tag{17}$$

6 Path Energy Bounds for Hub-Centric Graphs

In this section, we derive energy bounds for two distinct classes of graphs with order $k = 2n+1$ vertices: the hub-centric family, including closed helm, double star, friendship, and double wheel graphs. Our analysis specifically focuses on deriving lower and upper bounds for the path energy of these graphs, from the established generalized results (17). The methodology employed to derive these bounds is illustrated in a hierarchical, stepwise manner through the schematic diagram in Figure 3.

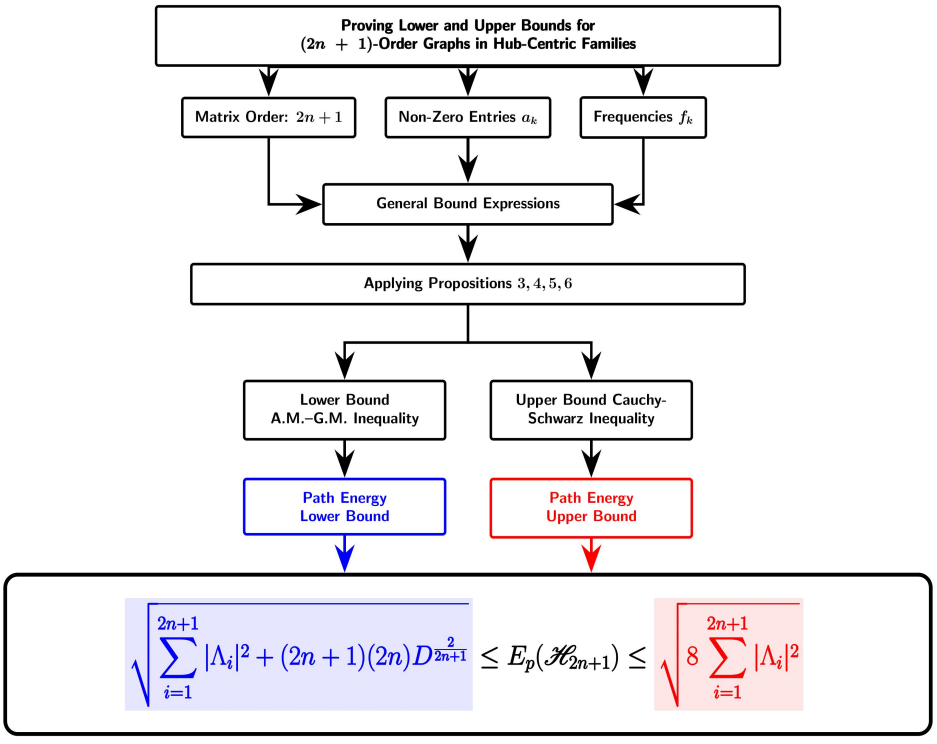

Figure 3: Schematic Illustration of Path Energy Bounds for $\mathscr{H}_{2n+1}$ graphs

6.1 Path Energy Bounds for Hub-Centric graphs ($\mathscr{H}_{2n+1}$)

Theorem 10. *For the closed helm graph CH_n with $n \geq 7$, and $k = 2n+1$ vertices, the path energy bounds of CH_n is as follows:*
Lower Bound:

$$E_p(CH_n) \geq \sqrt{16(n^2+n) + 9(3n^2+n) + (2n+1)(2n)D^{\frac{2}{2n+1}}} \tag{18}$$

Upper Bound:

$$E_p(CH_n) \leq \sqrt{8\big(16(n^2+n) + 9(3n^2+n)\big)} \tag{19}$$

Note: *By Proposition 3, it follows that $\sum_{i=1}^{k} \Lambda_i^2 = 16(n^2+n) + 9(3n^2+n)$, and applying (17), the bounds are derived and shown in Figure 4a.*

Theorem 11. *For the double star graph DS_n with $n \geq 3$, and $k = 2n+1$ vertices, the path energy bounds of DS_n is as follows:*
Lower Bound:

$$E_p(DS_n) \geq \sqrt{2n(2n+1) + (2n+1)(2n)D^{\frac{2}{2n+1}}} \tag{20}$$

Upper Bound:

$$E_p(DS_n) \leq \sqrt{8\big(2n(2n+1)\big)} \tag{21}$$

Note: *From Proposition 4, we have $\sum_{i=1}^{k} \Lambda_i^2 = 2n(2n+1)$, and using (17), the corresponding bounds are obtained and illustrated in Figure 5a.*

Theorem 12. *For the friendship graph F_n with $n \geq 6$, with $k = 2n+1$ vertices, the path energy bounds of F_n is as follows:*
Lower Bound:

$$E_p(F_n) \geq \sqrt{24n + 4n(n-1) + (2n+1)(2n)D^{\frac{2}{2n+1}}} \tag{22}$$

Upper Bound:

$$E_p(F_n) \leq \sqrt{8\big(24n + 4n(n-1)\big)} \tag{23}$$

Note: *From Proposition 5, we have $\sum_{i=1}^{k} \Lambda_i^2 = 24n + 4n(n-1)$, and using (17), the analytical bounds are derived. These bounds are depicted in Figure 6a. Friendship graph F_n, both the lower and improved lower bound of path energy parameters converges to the nearer values as n increases. The relation matrix structure becomes invertible, causing the determinant to approach zero. As a result, the lower bound closely approximates the improved lower bound for large n, which is evident from the Figure 6a in the plotted path energy.*

Theorem 13. *For the double wheel graph DW_n with $n \geq 3$, and $k = 2n+1$ vertices, the path energy bounds of DW_n is as follows:*
Lower Bound:

$$E_p(DW_n) \geq \sqrt{18n(n+1) + 2n^2 + (2n+1)(2n)D^{\frac{2}{2n+1}}} \tag{24}$$

Upper Bound:

$$E_p(DW_n) \leq \sqrt{8\big(18n(n+1) + 2n^2\big)} \tag{25}$$

Note: *From Proposition 6, we obtain $\sum_{i=1}^{k} \Lambda_i^2 = 18n(n+1) + 2n^2$, and using (17), the bounds are derived. These are shown in Figure 7a.*

7 Exact Bound for Path Energy of Hub-Centric Graphs $(\mathscr{H}_{2n+1})$

For a graph $\mathscr{H}_{2n+1}$ of order $2n+1$ with path adjacency matrix $A_p(\mathscr{H}_{2n+1})$, the exact path energy is

$$E_p\left(\mathscr{H}_{2n+1}\right) = \sum_{i=1}^{2n+1} |\Lambda_i|, \tag{26}$$

where $\Lambda_1, \ldots, \Lambda_{2n+1}$ are the eigenvalues are solving $|A_p\left(\mathscr{H}_{2n+1}\right) - \Lambda I| = 0$. The eigenvalues exhibit distinct multiplicity patterns due to the block structure of $A_p\left(\mathscr{H}_{2n+1}\right)$, specifically arising from the hub–rim connections. The matrix formulations established in Section 3 allow for the direct computation of these eigenvalues for each graph family.

Limitations. Among the considered $(2n+1)$-vertex graph families, only CH_n, and DS_n admit closed-form eigenvalue expressions, leading to exact path energy formulations. For the remaining F_n, and DW_n graphs. The eigenvalues do not follow a unified analytical pattern and vary with the vertex count n, making generalization difficult. So we derived the lower, improved lower, upper and improved upper bounds of such graphs. Consequently, their spectra must be determined individually for each n. Furthermore, the proposed framework is restricted to these specific structured $(2n+1)$-vertex graph families.

7.1 Path Energy Exact Bound for Closed Helm Graph CH_n

Theorem 14. *For the closed helm graph CH_n, $(n \geq 7)$, the exact path energy is $E_p(CH_n) = 7n - 3 + 39.46 + 6.54(n-6) - 0.46 + 0.46(n-6)$.*

Proof. The description of the path adjacency matrix of CH_n has been provided in Proposition 3, i.e.,

$$A_p(CH_n) = \begin{pmatrix} 4(J_{n+1} - I_{n+1}) & 3J_{(n+1)\times n} \\ 3J_{n\times(n+1)} & 3(J_n - I_n) \end{pmatrix}.$$

Solving the characteristic equation of this matrix $A_p(CH_n)$, the eigenvalues:

$$\Lambda_1 = \cdots = \Lambda_n = -4, \quad \Lambda_{n+1} = \cdots = \Lambda_{2n-1} = -3,$$
$$\Lambda_{2n} = (n-6)(6.54) + 39.46, \quad \Lambda_{2n+1} = (n-6)(0.46) - 0.46.$$

$$\text{Spec}\,(A_p(CH_n)) = \begin{bmatrix} -4 & -3 & (n-6)(6.54)+39.46 & (n-6)(0.46)-0.46 \\ n & n-1 & 1 & 1 \end{bmatrix}.$$

Therefore the exact path energy of CH_n is

$$\begin{aligned} E_p(CH_n) &= \sum_{i=1}^{2n+1} |\Lambda_i| \\ &= |-4|\,n + |-3|\,(n-1) + |(n-6)(6.54) + 39.46| \\ &\quad + |(n-6)(0.46) - 0.46| \\ &= 7n - 3 + 39.46 + 6.54(n-6) - 0.46 + 0.46(n-6). \end{aligned} \tag{27}$$

□

7.2 Path Energy Exact Bound for Double Star Graph DS_n

Theorem 15. *For the double star graph DS_n, $(n \geq 3)$, the exact path energy is $E_p(DS_n) = 4n$.*

Proof. The structure of the path adjacency matrix of DS_n has been already explained in Proposition 4, i.e.,

$$A_p(DS_n) = \begin{pmatrix} J_{n+1} - I_{n+1} & J_{(n+1)\times n} \\ J_{n\times(n+1)} & J_n - I_n \end{pmatrix}.$$

Solving the characteristic equation of $A_p(DS_n)$ yields the eigenvalues:

$$\Lambda_1 = \cdots = \Lambda_{2n} = -1, \quad \Lambda_{2n+1} = 2n.$$

$$\text{Spec}\,(A_p(DS_n)) = \begin{bmatrix} -1 & 2n \\ 2n & 1 \end{bmatrix}.$$

Hence, the exact path energy of DS_n is

$$E_p(DS_n) = \sum_{i=1}^{2n+1} |\Lambda_i| = |-1|(2n) + |2n|(1) = 2n + 2n = 4n. \tag{28}$$

□

8 Computational Approach for Hub-centric Graphs

The construction of the block-partitioned path adjacency matrix $A_p(\mathscr{H}_{2n+1})$ for hub-centric graphs are presented in **Algorithm** 1,2,3,4.

Algorithm 1 Path Energy and Time Complexity Analysis for CH_n

Input: $n \geq 7$ (integer, number of spokes)
Output: $E_p(CH_n)$ (path energy), avg/max/min execution times (seconds)
Complexity: $O((2n+1)^3)$ [QR eigenvalue algorithm]

Phase 1: Construct $(2n+1) \times (2n+1)$ **path matrix** A_p
$k \leftarrow 2n+1$ ▷ Total vertices
$A \leftarrow \mathbf{0}_{k\times k}$ ▷ Initialize zero matrix
for $i, j = 1$ to k, $i \neq j$ **do**
  if $i \leq n+1$ **and** $j \leq n+1$ **then**
    $A[i,j] \leftarrow 4$ ▷ Central hub+rim: 4 disjoint paths
  else
    $A[i,j] \leftarrow 3$ ▷ Outer rim/cross: 3 disjoint paths
  end if
end for
Phase 2: Path Energy analysis
Compute $\{\Lambda_1, \ldots, \Lambda_k\} \leftarrow \mathrm{eig}(A)$ ▷ QR algorithm, $O(k^3)$
Evaluate $E_p \leftarrow \sum_{i=1}^{k} |\Lambda_i|$ ▷ Path energy definition
Phase 3: Complexity measurement
Run independent trials for $n = 7$ to 200 ▷ Record avg/max/min times
return E_p, {avg, max, min} times

Complexity derivation: Matrix fill $O(k^2)$, eigendecomposition $O(k^3)$. Total: $O((2n+1)^3)$.
Validation: Python 3.9/NumPy on Intel i7 (32GB). $n = 7$: 0.02s avg; $n = 200$: 42.3s avg.

Algorithm 2 Path Energy and Time Complexity Analysis for DS_n

Input: $n \geq 3$ (integer, minimum vertex condition)
Output: $A_p(DS_n)$ (path energy), avg/max/min execution times (seconds)
Complexity: $O((2n+1)^3)$ [eigen decomposition]

Phase 1: Construct $(2n+1) \times (2n+1)$ **path matrix** A_p
$k \leftarrow 2n+1$ ▷ Total vertices
$A \leftarrow \mathbf{0}_{k\times k}$ ▷ Initialize zero matrix
for $i, j = 1$ to k, $i \neq j$ **do**
  $A[i,j] \leftarrow 1$ ▷ All off-diagonal entries represent exactly one internally vertex-disjoint path

5: **end for**
Phase 2: Path Energy analysis
6: $\{\Lambda_1, \ldots, \Lambda_k\} \leftarrow \text{eig}(A)$ ▷ QR algorithm, $O(k^3)$
7: $E_p \leftarrow \sum_{i=1}^{k} |\Lambda_i|$ ▷ Path energy
Phase 3: Complexity measurement
8: Run n trials for $n = 3$ to 200 ▷ Record average, maximum and minimum execution times
9: **return** E_p, {avg, max, min} times

Complexity derivation: Matrix construction $O(k^2)$, eigen decomposition $O(k^3)$. Total: $O((2n+1)^3)$.
Validation: Python 3.9/NumPy, Intel i7 (32GB RAM). $n = 3$: 0.001s avg; $n = 200$: 38.7s avg.

Algorithm 3 Path Energy and Time Complexity Analysis for F_n

Input: $n \geq 6$ (integer, number of triangles)
Output: $E_p(F_n)$ (path energy), avg/max/min execution times (seconds)
Complexity: $O((2n+1)^3)$ [eigen decomposition]

Phase 1: Construct $(2n+1) \times (2n+1)$ **path matrix** A_p
1: $k \leftarrow 2n+1$
2: $A \leftarrow \mathbf{0}_{k \times k}$
3: **for** $i = 1$ to k **do**
4: **for** $j = 1$ to k **do**
5: **if** $i = j$ **then**
6: $A[i, j] \leftarrow 0$
7: **else if** $i = 1$ or $j = 1$ **then**
8: $A[i, j] \leftarrow 2$
9: **else**
10: $A[i, j] \leftarrow 1$
11: **end if**
12: **end for**
13: **end for** ▷ Assign path value 2 to the paired peripheral vertices $(v_2, v_3), (v_4, v_5), \ldots, (v_{2n}, v_{2n+1})$
14: **for** $t = 2$ to $k - 1$ step 2 **do**
15: $A[t, t+1] \leftarrow 2$ $A[t+1, t] \leftarrow 2$
16: **end for**
Phase 2: Path Energy Analysis
17: $\{\Lambda_1, \Lambda_2, \ldots, \Lambda_k\} \leftarrow \text{eig}(A)$ ▷ $E_p(F_n) \leftarrow \sum_{i=1}^{k} |\Lambda_i|$
Phase 3: Complexity measurement
18: Run n trials for $n = 6$ to 200 ▷ Record avg/max/min execution times
19: **return** E_p, {avg, max, min} times

Complexity derivation: Matrix construction $O(k^2)$, eigen decomposition $O(k^3)$. Total: $O((2n+1)^3)$.
Validation: Python 3.9/NumPy on Intel i7 (32GB RAM). $n = 6$: 0.015s avg; $n = 200$: 41.2s avg.

Algorithm 4 Path Energy and Time Complexity Analysis for DW_n

Input: $n \geq 3$ (integer, rim size)
Output: $E_p(DW_n)$ (path energy), avg/max/min execution times (seconds)
Complexity: $O((2n+1)^3)$ [eigen decomposition]

Phase 1: Construct $(2n+1) \times (2n+1)$ **path matrix** A_p
$k \leftarrow 2n+1$
$A \leftarrow \mathbf{0}_{k \times k}$
for $i, j = 1$ to $n+1$ **do**
  if $i \neq j$ **then**
    $A[i,j] \leftarrow 3$
  end if
end for
for $i = n+2$ to k **do**
  for $j = n+2$ to k **do**
    if $i \neq j$ **then**
      $A[i,j] \leftarrow 3$
    end if
  end for
end for
for $i = 1$ to $n+1$ **do**
  for $j = n+2$ to k **do**
    $A[i,j] \leftarrow 1$
    $A[j,i] \leftarrow 1$
  end for
end for
Phase 2: Path Energy analysis
$\{\Lambda_1, \ldots, \Lambda_k\} \leftarrow \text{eig}(A)$ ▷ $E_p \leftarrow \sum_{i=1}^{k} |\Lambda_i|$
Phase 3: Complexity measurement
Run trials for $n = 3$ to 200 ▷ Record avg/max/min execution times
return E_p, {avg, max, min} times

Complexity derivation: Matrix construction $O(k^2)$, eigen decomposition $O(k^3)$. Total: $O((2n+1)^3)$.
Validation: Python 3.9/NumPy on Intel i7 (32GB RAM). $n = 3$: 0.008s avg; $n = 200$: 39.8 avg.

9 Numerical Comparison of Path Energy Bounds for Hub Centric Graphs

In this section, we compare our results with the classical bounds of Ilić and Bašić together with the most recent upper bound of Narke and Malavadkar.

9.1 Ilić–Bašić Lower Bound

Theorem 16 (Ilić–Bašić [14]). *For any connected graph G of order N,*

$$E_p(G) \geq 2(N-1). \tag{29}$$

Equality holds if and only if G is a tree.

For instance, considering this lower bound for the hub-centric graph with order $N = 2n+1$, and substituting into the above inequality yields

$$E_p(\mathscr{H}_{2n+1}) \geq 2\Big((2n+1)-1\Big) = 2(2n) = 4n.$$

Hence,

$$\boxed{E_p(\mathscr{H}_{2n+1}) \geq 4n.} \tag{30}$$

9.2 Ilić–Bašić Upper Bound

Theorem 17 (Ilić–Bašić [14]). *For any connected graph G of order N,*

$$E_p(G) \leq 2(N-1)^2. \tag{31}$$

Equality holds if and only if $G \cong K_N$.

Again, considering this upper bound for the hub-centric graph, using order $N = 2n+1$, and substituting into the above inequality yields

$$E_p(\mathscr{H}_{2n+1}) \leq 2\Big((2n+1)-1\Big)^2 = 2(2n)^2 = 8n^2.$$

Therefore,

$$\boxed{E_p(\mathscr{H}_{2n+1}) \leq 8n^2.} \tag{32}$$

9.3 Narke–Malavadkar (Degree Bassed) Upper Bounds

Theorem 18 (Narke–Malavadkar [19])**.** *Let G be a connected graph of order n with maximum degree Δ and $\mu = \min(n_+, n_-)$ is the minimum of the number of positive and negative eigenvalues, Then*

$$E_p(G) \leq 2\mu(N-1)\Delta. \tag{33}$$

For the hub-centric graph $\mathscr{H}_{2n+1}$,

$$\begin{aligned} E_p(\mathscr{H}_{2n+1}) &\leq 2\mu\Big((2n+1)-1\Big)\Delta \\ &= 2\mu(2n)\Delta = 4\mu n\Delta. \end{aligned}$$

Hence,

$$\boxed{E_p(\mathscr{H}_{2n+1}) \leq 4\mu n\Delta.} \tag{34}$$

Table 1: Comparison of Exact $E_p(CH_n)$ Values for the Closed Helm Graph with Existing and Proposed Bounds

n	**Exact Path Energy** $E_p(CH_n)$ (27)	**Existing Bounds**			**Proposed Bounds**	
		Ilić–Bašić Bounds		**Narke Bound**	**Lower Bound** (18)	**Upper Bound** (19)
		Lower Bound (30)	**Upper Bound** (32)	**Upper Bound** (34)		
8	106	32	512	512	80.9553	153.6750
50	694	200	20000	20000	496.3966	932.7379
100	1394	400	80000	80000	976.8961	1860.1075
150	2094	600	180000	180000	1455.8752	2787.4720
200	2794	800	320000	320000	1934.2620	3714.8351

Observation: The results presented in Theorem 9 demonstrate that the proposed upper bound is significantly tighter than the bounds obtained by Ilić–Bašić and Narke–Malavadkar. Furthermore, the proposed lower bound provides an effective estimate of the path energy, consistently remaining below the corresponding exact values. These observations confirm the validity and effectiveness of the derived bounds, as illustrated in Table 1.

Table 2: Comparison of Exact $E_p(DS_n)$ Values for the Double Star Graph with Existing and Proposed Bounds

n	**Exact Path Energy** $E_p(DS_n)$ (28)	**Existing Bounds**			**Proposed Bounds**	
		Ilić–Bašić Bounds		**Narke Bound**	**Lower Bound** (20)	**Upper Bound** (21)
		Lower Bound (30)	**Upper Bound** (32)	**Upper Bound** (34)		
8	32	32	512	256	25.4736	46.6476
50	200	200	20000	10000	145.4797	284.2534
100	400	400	80000	40000	287.3607	567.0979
150	600	600	180000	90000	429.0547	849.9412
200	800	800	320000	160000	570.6711	1132.7842

Observation: The Double Star graph exhibits the simplest structure with all off-diagonal entries equal to 1. Our bounds derived in Theorem 10 are remarkably tight compared to general bounds. The exact formula $E_p(DS_n) = 4n$ is captured well by our upper bound $\sqrt{8 \cdot 2n(2n+1)}$ as illustrated in Table 2

Table 3: Comparison of Exact $E_p(F_n)$ Values for the Friendship Graph with Existing and Proposed Bounds

n	**Exact Path Energy** $E_p(F_n)$ (26)	**Existing Bounds**			**Proposed Bounds**	
		Ilić–Bašić Bounds		**Narke Bound**	**Lower Bound** (22)	**Upper Bound** (23)
		Lower Bound (30)	**Upper Bound** (32)	**Upper Bound** (34)		
8	38.6274	32	512	512	20.3961	57.6888
50	207.7033	200	20000	20000	104.8809	296.6479
100	407.8461	400	80000	80000	204.9390	579.6551
150	607.8961	600	180000	180000	304.9590	862.5543
200	807.9216	800	320000	320000	404.9691	1145.4257

Observation: Friendship graphs exhibit intermediate complexity and its bounds are obtained in Theorem 11. The upper bound is considerably tighter than the general bounds, with a tightness ratio of approximately 1.44 relative to the exact values, while the lower bound provides a conservative estimate, as shown in Table 3.

Table 4: Comparison of Exact $E_p(DW_n)$ Values for the Double Wheel Graph with Existing and Proposed Bounds

n	**Exact Path Energy** $E_p(DW_n)$ (26)	**Existing Bounds**			**Proposed Bounds**	
		Ilić–Bašić Bounds		**Narke Bound**	**Lower Bound** (24)	**Upper Bound** (25)
		Lower Bound (30)	**Upper Bound** (32)	**Upper Bound** (34)		
8	92.6431	32	512	1024	73.8567	106.7333
50	596.9345	200	20000	40000	396.9569	638.1222
100	1196.9667	400	80000	160000	774.2099	1270.5904
150	1796.9777	600	180000	360000	1150.2005	1903.0502
200	2396.9833	800	320000	640000	1525.6723	2535.5078

Observation: Double Wheel graphs represent the most complex structure among the four families, requiring three disjoint paths in multiple regions. Despite this complexity the bounds are established in Theorem 12, our upper bound remains within a factor of 1.42 of the exact values, demonstrating the effectiveness as depicted in Table 4.

Remark 19. *The inequality in* (35) *provides a complete comparison framework for the path energy bounds of* $\mathscr{H}_{2n+1}$. *The proposed bounds lie between the classical estimates of Ilić and Narke, yielding a refined enclosure of* $E_p(\mathscr{H}_{2n+1})$.

This highlights improved spectral localization through explicit eigenvalue-dependent bounds.

$$\begin{aligned} 4n \;\le\; \sqrt{\sum_{i=1}^{2n+1} |\Lambda_i|^2 + (2n+1)(2n)\, D^{\frac{2}{2n+1}}} \;\le\; E_p(\mathscr{H}_{2n+1}) \\ \le\; \sqrt{8\sum_{i=1}^{2n+1} |\Lambda_i|^2} \;\le\; 2\mu(2n)\Delta \;\le\; 8n^2. \end{aligned} \tag{35}$$

10 Graphical Representation Path Energy Bounds of Hub-Centric Graphs

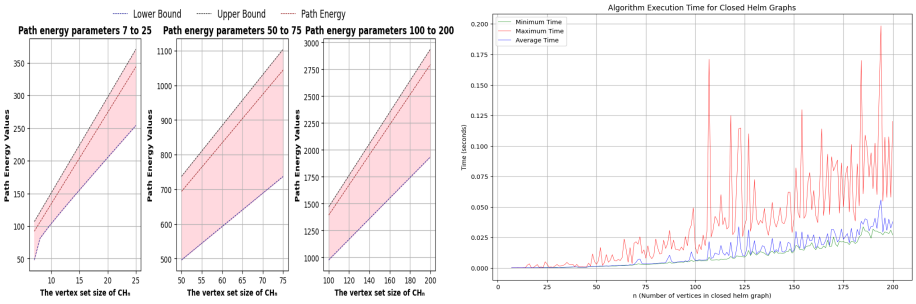

(a) Path Energy Bounds of Closed Helm (b) Algorithm Execution Time of Closed Helm

Figure 4: Bounds of Closed Helm (a) and its Algorithm Execution Time (b)

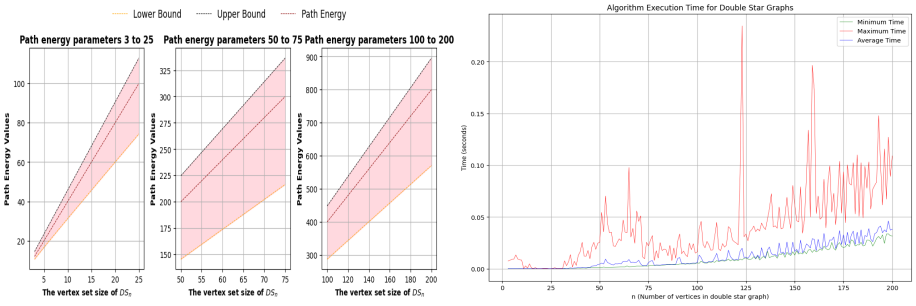

(a) Path Energy Bounds of Double Star (b) Algorithm Execution Time of Double Star

Figure 5: Bounds of Double Star (a) and its Algorithm Execution Time (b)

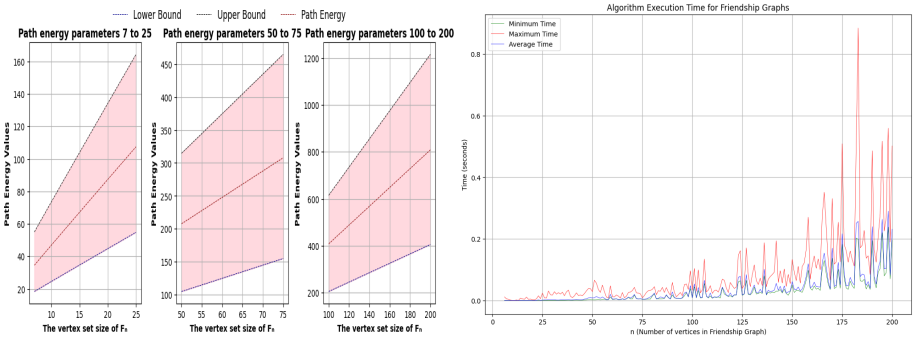

(a) Path Energy Bounds of Friendship (b) Algorithm Execution Time of Friendship

Figure 6: Bounds of Friendship (a) and its Algorithm Execution time (b)

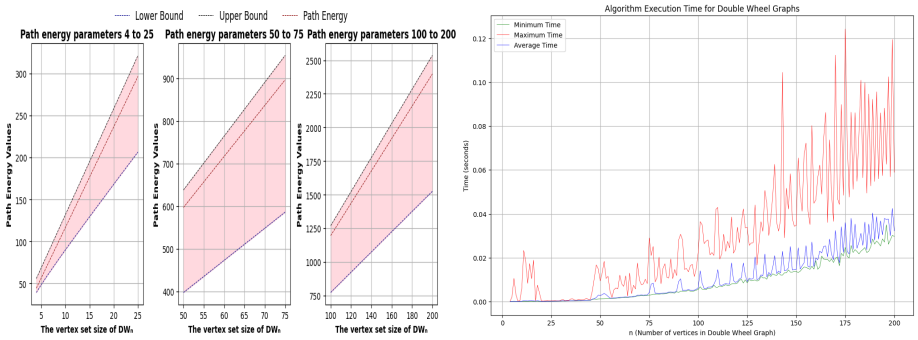
Lower Bound
Upper Bound
Path Energy
Path energy parameters 4 to 25
Path energy parameters 50 to 75
Path energy parameters 100 to 200
Path Energy Values
The vertex set size of DW
Algorithm Execution Time for Double Wheel Graphs
Minimum Time
Maximum Time
Average Time
Time (seconds)
n (Number of vertices in Double Wheel Graph)

(a) Path Energy Bounds of Double Wheel (b) Algorithm Execution Time of Double Wheel

Figure 7: Bounds of Double Wheel (a) and its Algorithm Execution Time (b)

11 Complexity Analysis of $(2n+1)$-Hub Centric Graphs

We conducted a detailed computational analysis of four $(2n+1)$-vertex hub centric graphs, by applying algorithms of the four graphs. This algorithmic approach helps to quantify both the energy of these graphs and the computation time required for each calculation. The execution time taken to run each of these algorithms determines the complexity nature of these $2n+1$ graphs. Higher the computational time infers higher complexity nature of the $2n+1$ graphs. By plotting energy against computation time as shown in Figure 8, we rigorously evaluated the inherent complexity and efficiency of each graph type. Our findings indicate that friendship graphs display notably higher complexity relative to other $(2n+1)$-graphs analyzed. Furthermore, the comparative numerical tables presented for all four hub centric graphs demonstrate that the proposed lower and upper bounds are consistently and substantially tighter than the corresponding bounds of Ilić–Bašić and Narke–Malavadkar. This improved tightness confirms the effectiveness and accuracy of the derived estimates across the entire range of graph parameters considered. In particular, the computational time for friendship graphs follows a complexity of $O(n^3)$, emphasizing its critical computational demands in the context of the $(2n+1)$-graphs examined in this study.

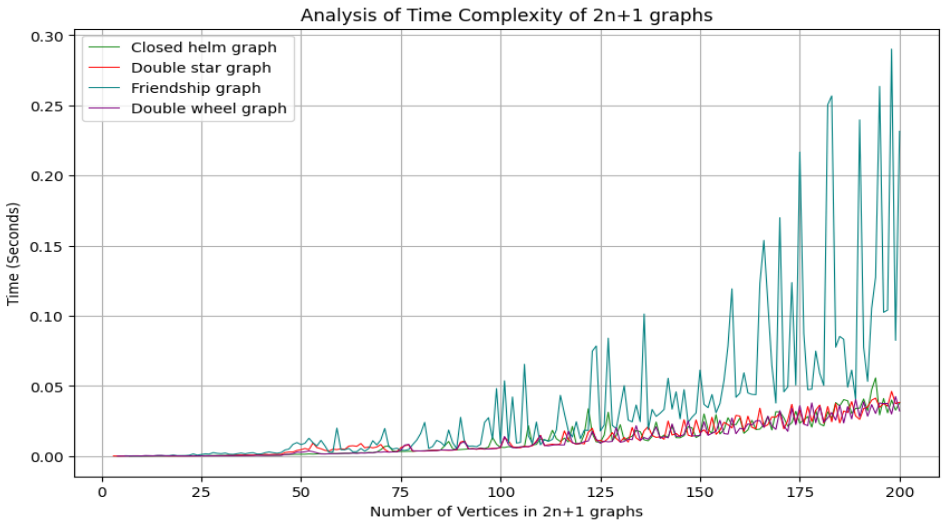

Figure 8: Analysis of time complexity of (2n+1)-graphs

12 Conclusion

This paper provides a computational framework for evaluating path energy in $(2n+1)$-vertex hub centric topology, emphasizing their unique advantages in real-world applications. The inherent asymmetry of $(2n+1)$-networks provides a significant edge in addressing complex network challenges. In **power grids** [25], fault-tolerant path ensure uninterrupted energy distribution during failures, enhancing system reliability. In **satellite networks**, their asymmetrical structure supports robust communication paths, maintaining stable data transmission despite link disruptions. Similarly, in **IoT sensor networks** [1], $(2n+1)$-network structure enables the design of energy-efficient and fault-resilient systems, ensuring consistent data flow while minimizing downtime. By delivering precise pathway energy bounds and efficient computational methods, this paper demonstrates that $(2n+1)$-graphs are particularly well-suited for optimizing asymmetrical and fault-tolerant networks, surpassing the capabilities of $2n$-graphs. The core contribution of this work lies in the improved efficiency and adaptability of paths energy computations, offering a powerful tool for tackling intricate spectral graph problems. These results lay the foundation for future research, including optimizing algorithms and exploring new graph families.

References

[1] Kiki Adhinugraha, Wenny Rahayu, Takahiro Hara, and David Taniar. Measuring fault tolerance in IoT mesh networks using Voronoi diagram. *Journal of Network and Computer Applications*, 199:103297, 2022. doi:10.1016/j.jnca.2021.103297.

[2] Chandrashekar Adiga, E. Sampathkumar, M. A. Sriraj, and A. S. Shrikanth. Color energy of a graph. *Proceedings of the Jangjeon Mathematical Society*, 16(3):335–351, 2013.

[3] Saieed Akbari, Abdullah Alazemi, Milica Andelić, and Mohammad Ali Hosseinzadeh. On the energy of line graphs. *Linear Algebra and its Applications*, 636:143–153, 2022. doi:10.1016/j.laa.2021.11.022.

[4] Saieed Akbari, Maryam Ghahremani, Mohammad Ali Hosseinzadeh, Somayeh Khalashi Ghezelahmad, Hamid Rasouli, and Abolfazl Tehranian. A lower bound for graph energy in terms of minimum and maximum degrees. *MATCH Communications in Mathematical and in Computer Chemistry*, 86(3):549–558, 2021.

[5] R. Balakrishnan and K. Ranganathan. *A Textbook of Graph Theory*. Universitext. Springer New York, 2nd edition, 2012. doi:10.1007/978-1-4614-4529-6.

[6] Ş. Burcu Bozkurt Altındağ, Emina Milovanović, Marjan Matejić, and Igor Milovanović. Remarks on the bounds of graph energy. *Communications in Combinatorics and Optimization*, 11(1):211–226, 2026. doi:10.22049/cco.2024.28825.1739.

[7] Yirui Chai, Ligong Wang, and Yuwei Zhou. D-integral, D^Q-integral and D^L-integral generalized double-wheel graphs. *Bulletin of the Malaysian Mathematical Sciences Society*, 47(4):118, 2024. doi:10.1007/s40840-024-01710-7.

[8] Zdravko Cvetkovski. *Inequalities: Theorems, Techniques and Selected Problems*. Springer Berlin, Heidelberg, 2012. doi:10.1007/978-3-642-23792-8.

[9] Szymon Duraj, Paweł Kopeć, Marek Kubale, and Tytus Pikies. Scheduling of identical jobs with bipartite incompatibility graphs on uniform

machines. computational experiments. *Decision Making in Manufacturing and Services*, 11(1-2):53–61, 2017. doi:10.7494/dmms.2017.11.1-2.53.

[10] Ivan Gutman. Graph energy and nullity. *Open Journal of Discrete Applied Mathematics*, 4(1):25–28, 2021. doi:10.30538/psrp-odam2021.0051.

[11] Ivan Gutman and Boris Furtula. Survey of graph energies. *Mathematics Interdisciplinary Research*, 2(2):85–129, 2017. doi:10.22052/mir.2017.81507.1057.

[12] Ivan Gutman and Harishchandra S. Ramane. Research on graph energies in 2019. *MATCH Communications in Mathematical and in Computer Chemistry*, 84(2):227–292, 2020.

[13] Frank Hutter, Lin Xu, Holger H. Hoos, and Kevin Leyton-Brown. Algorithm runtime prediction: Methods & evaluation. *Artificial Intelligence*, 206:79–111, 2014. doi:10.1016/j.artint.2013.10.003.

[14] Aleksandar Ilić and Milan Bašić. Path matrix and path energy of graphs. *Applied Mathematics and Computation*, 355:537–541, 2019. doi:10.1016/j.amc.2019.03.002.

[15] P. Kowsalya and D. Vijayalakshmi. On radio k –chromatic number for Mycielski of some graphs. *Indian Journal of Science and Technology*, 17(39):4129–4137, 2024. doi:10.17485/IJST/v17i39.2315.

[16] Xueliang Li, Yongtang Shi, and Ivan Gutman. *Graph Energy*. Springer New York, 2012. doi:10.1007/978-1-4614-4220-2.

[17] Igor Mezić, Vladimir A. Fonoberov, Maria Fonoberova, and Tuhin Sahai. Spectral complexity of directed graphs and application to structural decomposition. *Complexity*, 2019(1):9610826, 2019. doi:10.1155/2019/9610826.

[18] Aleksa Milojević. Connectivity of old and new models of friends-and-strangers graphs. *Advances in Applied Mathematics*, 155:102668, 2024. doi:10.1016/j.aam.2023.102668.

[19] Amol P. Narke and Prashant P. Malavadkar. An efficient algorithm for path matrix computation and improved path energy bounds. In

Christos Zaroliagis, Dinabandhu Bhandari, Prosenjit Gupta, and Swagatam Das, editors, *Proceedings of the International Conference on Applied Algorithms (ICAA 2026)*, volume 16423 of *Lecture Notes in Computer Science*, pages 15–25, Cham, 2026. Springer Nature Switzerland. doi:10.1007/978-3-032-15621-1_2.

[20] S. C. Patekar and M. M. Shikare. On the path energy of some graphs. *Journal of Mathematical and Computational Science*, 10(3):535–543, 2020. doi:10.28919/jmcs/4460.

[21] Ali Raza, Muhammad Mobeen Munir, Tasawar Abbas, Sayed Eldin, and Ilyas Khan. Spectrum of prism graph and relation with network related quantities. *AIMS Mathematics*, 8(2):2634–2647, 2023. doi:10.3934/math.2023137.

[22] Maruti M. Shikare, Prashant P. Malavadkar, Shridhar C. Patekar, and Ivan Gutman. On path eigenvalues and path energy of graphs. *MATCH Communications in Mathematical and in Computer Chemistry*, 79(2):387–398, 2018.

[23] P. N. Simha, B. P. Shylaja, N. Narahari, H. M. Nagesh, and U. V. C. Kumar. On the distribution of vertex energy of connected non-regular non-bipartite integral graphs with maximum vertex degree four. *Scientific Annals of Computer Science*, 35(2):197–210, 2025. doi:10.47743/SACS.2025.2.197.

[24] Johan Simonsson, Khalid Tourkey Atta, and Wolfgang Birk. A graph theoretical approach to modeling of district energy networks. *IEEE Transactions on Control Systems Technology*, 32(5):1616–1630, 2024. doi:10.1109/TCST.2023.3345213.

[25] Anurag K. Srivastava, Timothy A. Ernster, Ren Liu, and Vignesh G. Krishnan. Graph-theoretic algorithms for cyber-physical vulnerability analysis of power grid with incomplete information. *Journal of Modern Power Systems and Clean Energy*, 6(5):887–899, 2018. doi:10.1007/s40565-018-0448-7.

[26] Leyou Xu and Bo Zhou. The path-index of a graph. *Applied Mathematics and Computation*, 461:128312, 2024. doi:10.1016/j.amc.2023.128312.

[27] Luzhen Ye. On the energy of a graph and its edge-deleted subgraphs. *MATCH Communications in Mathematical and in Computer Chemistry*, 92(2):417–423, 2024. doi:10.46793/match.92-2.417Y.

© Scientific Annals of Computer Science 2026